

1

2

3

4

5

ICOS enhances follicular T helper responses and deteriorates the pathogenic process of liver in mice infected with *Schistosoma japonicum*

6

7 Bo Wang^{1,2}, Song Liang², Yan-Yan Wang², Yu Wang², Chao-Ming Xia^{2*}

8

1 Laboratory Department, Inner Mongolia People's Hospital, Huhhot, Inner Mongolia Autonomous

9

Region, The Peoples Republic of China, 010017

10

2 Department of Parasitology, Medical College of Soochow University, Suzhou, Jiangsu Province, The

11

Peoples Republic of China, 215123

12

13 * Corresponding author: Professor Chao-Ming Xia, Department of Parasitology, Medical

14 College of Soochow University, Renai Road, Industrial Park, Suzhou 215123, Jiangsu

15 Province, P. R. China.

16 E-mail: cmx2019@126.com

17 **Funding:** This work was supported by grants from the National Natural Science Foundation

18 of China (No: 81171603 and No: 81471977) to C.M.X and the General Program of Inner

19 Mongolia Natural Science Foundation of China (No:2016BS0812), A project funded by the

20 Program of Inner Mongolia People's Hospital Foundation (No:2019YN23) to B.W. The

21 funders had no role in study design, data collection and analysis, decision to publish, or

22 preparation of the manuscript.

23 **Abstract**

24 **Background:** Humoral immune responses play an important role in mediating liver
25 granulomatous inflammation and fibrosis in schistosomiasis. Follicular helper T (Tfh) cells
26 have a central role in mediating humoral immune responses. Generation of Tfh cells depends
27 on inducible T cell costimulator (ICOS) signaling, but the underlying molecular mechanisms
28 are incompletely understood in pathogenesis of schistosomiasis.

29 **Methodology/Principal Findings:** We used a strain of ICOS-transgenic (Tg) mice to
30 test the degrees of liver granulomatous inflammation and fibrosis, the frequency of splenic
31 Tfh cells and soluble egg antigen-specific cytokine responses longitudinally in mice
32 following *Schistosoma japonicum* (*S. japonicum*) infection. In comparison with that in
33 wide-type (WT) mice, significantly severer liver granulomatous inflammation and fibrosis
34 and higher mortality were observed in ICOS-Tg mice. Significantly higher frequency of
35 splenic Tfh cells was accompanied by significantly higher levels of Bcl-6 and CXCR5
36 expression in the livers of ICOS-Tg mice. Furthermore, significantly higher levels of
37 SEA-specific IL-4, IL-6, IL-10, IL-13, IL-17A, IL-21 and TGF- β 1 responses, but lower
38 levels of IFN- γ responses were detected in ICOS-Tg mice, which were abrogated by
39 treatment with ICOS blockers in vitro. In addition, significantly higher levels of serum
40 anti-SEA IgG were detected in ICOS-Tg mice.

41 **Conclusions/Significance:** The ICOS-related signaling may promote the pathogenesis
42 of murine schistosomiasis by polarizing Tfh cells, which may be immune check points for the
43 prevention and intervention of schistosomiasis.

44 **Author summary**

45 Granulomatous inflammation and fibrosis in the liver are the major pathogenic
46 characteristics of schistosomiasis. ICOS is crucial for the development of Tfh cells, which are
47 the key modulators of B cell activation and humoral immunity. However, the underlying
48 molecular mechanisms are incompletely understood in pathogenesis of schistosomiasis. Here,
49 our results showed that the ICOS over-expression would significantly induce severer liver
50 inflammation and fibrosis, higher frequency of splenic Tfh, higher levels of anti-SEA IgG as
51 well as imbalanced SEA-specific cytokine responses in ICOS-Tg mice. The findings
52 suggested that ICOS signaling may promote the pathogenesis of murine schistosoma-related
53 liver inflammation and fibrosis by polarizing Tfh cells. Potentially, ICOS signaling and Tfh
54 cells may be immune check points for the prevention and intervention of schistosomiasis.

55

56 **Introduction**

57 *S. japonicum* infection remains a problem for human health in developing countries.
58 During the pathogenesis of schistosomiasis, *S. japonicum* infection-related egg deposition can
59 recruit inflammatory infiltrates and cause granulomatous inflammation and fibrosis in the
60 liver [1,2]. More importantly, continual pathogenic process of inflammation and fibrosis in
61 the liver usually impairs its function, even leading to cirrhosis and live failure. Although
62 previous studies have shown that antigen-specific T cells, such as Th2 and Th17, participate
63 in the pathogenic process and Th1 and regulatory T cells (Tregs) antagonize *Schistosomiasis*-
64 related inflammation [3-5]. The molecular mechanisms of immunoregulation of *S. japonicum*
65 infection-related inflammation and fibrosis in the liver have been incompletely clarified.
66 Hence, illustration of the pathogenic process of *S. japonicum* infection-related inflammation
67 and fibrosis will be of great significance in the develop targets for design of new therapies for
68 patients with schistosomiasis.

69 Tfh cells are activated CD4⁺ T cells commonly resident in the B cell follicles of second
70 lymph tissues and constitutively express homing receptor CXCR5 [6,7]. Tfh cells can also
71 express programmed death 1 (PD-1), ICOS and CD40L and secrete IL-21 as well as other
72 cytokines, which are crucial for their autocrine regulation of Tfh development and functions
73 [8-10]. Tfh differentiation is mainly regulated by the transcription factor, Bcl-6 [11].Tfh cells
74 can promote antigen-specific B cell activation, germinal center formation and humoral
75 responses [12,13]. In addition, Tfh cells are involved in the pathogenic process of some
76 autoimmune diseases [14-16] and participate in defending against parasite infection [17,18].
77 Indeed, increased frequency of Tfh cells is detected in rodent with *S. japonicum* infection and

78 Tfh cells activated by ICOS⁺ macrophages infiltrate into the liver and enhance the liver injury
79 in mice infected with *S. japonicum* [19].

80 ICOS is crucial for T and B cell activation and important for T and B cell interaction to
81 promote humoral responses [20]. ICOS is highly expressed by human tonsillar CXCR5⁺ T
82 cells within the light zone of germinal centers and efficiently support immunoglobulin
83 production [21,22]. In addition, ICOS-deficient mice show poor humoral responses and ICOS
84 deficiency in humans results in significantly reduced numbers of Tfh cells, indicating a
85 critical role of ICOS in the differentiation of CXCR5⁺ CD4⁺ T cells [23,24]. However, it is
86 incompletely understood that the underlying molecular mechanisms of Tfh development and
87 function in pathogenesis of schistosomiasis. Here we characterized to establish the ICOS-Tg
88 mice as a model of schistosomiasis to assess the role of the ICOSL/ICOS interaction in
89 mediating humoral immune responses by polarizing Tfh cells, particularly, which were
90 abrogated by treatment with ICOS blockers in vitro. ICOS signaling and Tfh cells may be
91 immune check points for the prevention and intervention of schistosomiasis.

92

93 **Methods**

94 **Ethics statement**

95 The experimental protocols were established, according to the Regulations for the
96 Administration of Affairs Concerning Experimental Animals (1988.11.1) of the State Science
97 and Technology Commission of the People's Republic China and were approved by the
98 Institutional Animal Care and Use Committee (IACUC) of Soochow University (Permit
99 Number: 2007-13). All efforts were made to minimize suffering of animals.

100

101 **Mice, parasites, and infection**

102 Specific pathogen-free (SPF) female FVB mice (6-8 weeks old) were purchased from
103 the Center of Comparative Medicine of Yangzhou University (Yangzhou, China). Animals
104 were housed and bred in a SPF facility of our campus. To generate ICOS-Tg mice, human
105 ICOS cDNA was amplified by RT-PCR from activated human T cells and cloned into a
106 vector pEGFP-N2 plasmid, and a Tg cassette that drives transgene expression by the CMV
107 promoter/enhancer. The *AseI-StuI* transgene fragment at 0.642 kb was microinjected into
108 fertilized mouse eggs prepared from FVB mice.

109 The generated ICOS-Tg founders were backcrossed to FVB mice over 10 generations to
110 stabilize the Tg strain (Yangzhou, China). Snails (*Oncomelania hupensis*) harboring *S.*
111 *japonicum* cercariae (Chinese mainland strain) were purchased from Jiangsu Institute for
112 Schistosomiasis Control (Wuxi, China).

113 Individual FVB wide-type and ICOS-Tg mice at 6-8 weeks of age were infected with
114 14 (\pm 1) cercaria of *S. japonicum* through the abdominal skin. At 4, 7, 12, 16, and 20 weeks
115 post-infection, 8 mice at each time point from the infected and control groups were randomly
116 chosen and sacrificed for subsequent *ex vivo* experiments. The remaining 20 mice per group
117 were monitored for their survival until they met certain clinical criteria for sacrifice. The
118 criteria included severe diarrhea, and difficult to eat and breath.

119

120 **Flow cytometry**

121 The frequency of T_{fh} and other subsets of T cells was determined by flow cytometry

122 analysis. Briefly, splenic mononuclear cells were prepared from individual mice at each time
123 point post infection and the cells at 1×10^6 /tube were stained in duplicate with FITC-anti-CD4,
124 PE-anti-CXCR5, PE-Cy5-anti-ICOS, and APC-anti-CD40L or isotype controls (eBioscience,
125 San Diego, USA). The percentages of CXCR5⁺CD4⁺ Tfh cells, ICOS⁺CXCR5⁺CD4⁺ Tfh
126 cells and CD40L⁺CXCR5⁺CD4⁺ Tfh cells were analyzed on a FACS Calibur Flow Cytometer
127 (BD Biosciences).

128 In addition, splenic mononuclear cells at 1×10^6 cells/well were stimulated with 25
129 ng/ml of phorbolmyristate acetate (PMA) and 1 μ g/ml of ionomycin (Sigma-Aldrich) in
130 complete RPMI 1640 medium in the presence of 3 μ g/ml of BFA for 5 hours at 37 °C in 5%
131 CO₂. Subsequently, the cells were surface-stained with FITC-anti-CD4 and PE-anti-CXCR5
132 or FITC-anti-CD4 alone, fixed, permeabilized with Fixation/Permeabilization buffer,
133 followed by intracellularly staining with APC-anti-IL-21, PE-anti-BCL-6 or isotype controls
134 for analyzing the frequency of IL-21⁺CXCR5⁺CD4⁺ or BCL-6⁺CD4⁺ Tfh cells, respectively.

135

136 **Culture and stimulation of splenic mononuclear cells *in vitro***

137 Splenic mononuclear cells were prepared from individual mice in each group at the
138 indicated time points post infection. Splenic mononuclear cells at 1×10^6 cells/well were
139 stimulated in triplicate with 25 μ g/ml of soluble egg antigens (SEA) of *S. japonicum* from
140 Jiangsu Institute for Schistosomiasis Control (Wuxi, China), 25 ng/ml of PMA and 1 μ g/ml of
141 ionomycin in 10% fetal bovine serum (FBS) RPMI 1640 in 24-well plates at 37 °C for 72
142 hours in the presence or absence of 0.5 μ g/ml of anti-ICOSL or 0.375 μ g/ml of antagonist
143 anti-ICOS (eBioscience). The culture supernatants were collected and the contents of

144 cytokines (IL-2, IL-4, IL-6, IL-10, IL-13, IL-17A, IL-21, IFN- γ , TNF- α) were determined by
145 Cytometric Bead Array (CBA) using specific kit (BD Biosciences, San Diego, USA),
146 according to the manufacturers' instruction. The levels of TGF- β 1 in the cultured supernatants
147 were measured by ELISA using the ELISA Ready-SET-Go kit (eBioscience, San Diego, CA),
148 according to the manufacturers' protocol. The limitation of detection for IL-2, IL-4, IL-6,
149 IL-10, IL-13, IL-17A, IL-21, IFN- γ , TNF- α and TGF- β 1 is (2.8pg/ml) respectively.

150

151 **Enzyme-linked immunosorbent assay (ELISA)**

152 The concentrations of serum SEA-specific IgG and HA in individual mice were
153 evaluated by ELISA. Briefly, individual wells of 96-well ELISA plates (ICN Biomedicals,
154 Costa Mesa, USA) were coated with 100 μ l of SEA (20 μ g/ml) in 0.05 M carbonate buffer
155 (pH 9.6) overnight at 4°C and after being washed and blocked with 10% FCS in 0.01M PBST,
156 the wells were added in triplicate with 1:100 diluted serum samples and cultured at 37 °C for
157 1 hour. The bound antibodies were detected with horseradish peroxidase (HRP)-conjugated
158 goat anti-mouse IgG (1:4000) for 1 hour at 37 °C and developed with tetramethyubenzidine
159 (TMB) substrate (BD PharMigen), followed by measuring the absorbance of individual wells
160 at 450 nm using an ELISA reader (Bio-rad mod.550). Serum samples from unmanipulated
161 mice were used for negative controls.

162

163 **Histopathological study**

164 The liver tissue samples from individual mice were dissected out at the indicated time
165 points post infection, fixed with paraformaldehyde and paraffin-embedded. The tissue

166 sections at 5 μm were stained with hematoxylin-eosin and the egg-related granuloma volumes
167 of individual liver samples were evaluated using a formula of $V=\pi AB^2/6$, where A and B
168 represented two diameters cross opposite axes [5].

169 Furthermore, some liver tissue sections were stained with Masson trichrome (MT). The
170 degrees of liver fibrosis in at least 10 low-power fields (magnification x 100) of each sample
171 were evaluated by pathologists in a blinded manner. In addition, the percentages of collagen+
172 regions were calculated using an image analysis system (Image-Pro Plus 6.0) to measure a
173 relative objective index. The fibrotic areas were calculated and expressed as the relative ratios
174 of the collagen-containing area to the whole area. At least 10 high-power fields
175 (magnification x 200) were measured from each liver sample.

176

177 **Immunohistochemistry**

178 The contents of CXCR5 and Bcl-6 expression in the livers of individual mice were
179 evaluated by immunohistochemistry. Briefly, liver tissue sections (5 μm) were rehydrated,
180 and treated with 3% H_2O_2 , followed by blocking with 10% normal goat serum (Boster,
181 Wuhan, China). Subsequently, the sections were incubated with rabbit anti-CXCR5 (1:500,
182 Millipore, Germany) or rabbit anti-Bcl-6 (1:100, Santa Cruz, USA) overnight at 4 °C and
183 bound antibodies were detected using HRP-conjugated goat anti-rabbit IgG (ChemMate
184 Envision/HRP, rabbit/mouse detection kit, Gene-tech, Shanghai, China) at 37 °C for 1 hour.
185 After being washed, the immune staining was visualized using 3, 3'-Diaminobenzidine (DAB)
186 and counterstained with Mayer's hematoxylin. Rabbit sera at 1:10 dilutions served as
187 negative controls. The intensity and percentages of positive staining cells in the liver

188 granulomas were evaluated for five high-power fields selected randomly using the Leica
189 QWin Plus software, version 3.5.1 (Leica Microsystems, Switzerland). The percentage of
190 positively staining cells in 15 granulomas was assessed and the mean of % positively staining
191 cells in 15 granulomas +/- SD in each group was calculated.

192

193 **Statistical analysis**

194 Statistical analysis was performed using the SPSS version 10.1 (Statistical Package for
195 Social Science, Chicago, IL) software. The difference of the data among the groups was
196 compared by two-way ANOVA followed by Tukey's multiple comparison test. The
197 relationship between measures was analyzed by Spearman's rank correlation. The survival of
198 each group of mice was estimated by Kaplan-Meier survival analysis and the difference
199 between two groups was analyzed by the log-rank test. A P value of $P < 0.05$ were considered
200 statistically significant.

201

202 **Results**

203 **ICOS over-expression deteriorates the liver granulomatous inflammation and fibrosis in** 204 **mice post-infection**

205 *S. japonicum* infection can cause liver granulomatous inflammation and fibrosis. To
206 assess the impact of ICOS over-expression on *S. japonicum* infection-related liver
207 inflammation the liver and spleen gross pathology, weights and liver granulomatous
208 inflammation were examined longitudinally in WT and ICOS-Tg mice following *S.*
209 *japonicum* infection. We observed dark-yellow livers (Fig 1A-b,c) compared with

210 non-infected liver (Fig 1A-a) and enlarged spleens in the mice infected with *S. japonicum*
211 (Fig 1A-d). The liver and spleen weights in the mice infected with *S. japonicum* rapid
212 increased and significantly greater than that in the non-infected mice (Fig 1B). The liver and
213 spleen weights in ICOS-Tg mice were significantly greater than that in the WT mice at 4
214 weeks post infection and later time points (Fig 1B; * $P < 0.05$ or ** $P < 0.01$). Histological
215 examination indicated that the mean volumes of granulomas in the ICOS-Tg mice were also
216 significantly bigger than that in the WT mice (Fig 1C and D). More importantly, the overall
217 survival periods of ICOS-Tg mice were significantly shorter than that in the WT mice (Fig 1E;
218 $P < 0.01$). Collectively, these data indicated that induction of systemic ICOS over-expression
219 deteriorated the liver granulomatous inflammation and fibrosis and accelerated mortality in
220 mice infected with *S. japonicum*.

221 Given that chronic *S. japonicum* infection is associated with the liver fibrosis we
222 examined the effects of systemic ICOS over-expression on the liver fibrosis in mice infected
223 with *S. japonicum*. MT staining revealed that the liver fibrosis developed at 7 weeks post
224 infection and the degrees of liver fibrosis increased with time in mice following *S. japonicum*
225 infection (Fig 2A). Quantitative analysis pointed out that the degrees of liver fibrosis in the
226 ICOS-Tg mice were significantly greater than that in the WT mice (Fig 2B; $P < 0.01$).
227 Therefore, induction of systemic ICOS over-expression enhanced the fibrotic process in the
228 livers of mice following *S. japonicum* infection.

229

230 **Fig 1. Hepatic granulomatous inflammation and fibrosis in ICOS-Tg mice post-infection.**

231 Female FVB ICOS-Tg and WT mice were infected with *S. japonicum*. The liver and spleen

232 gross pathology, weights and liver granulomatous inflammation in WT and ICOS-Tg mice
233 were examined longitudinally at the indicated time points post *S. japonicum* infection. The
234 liver tissue sections were stained with H&E and granulomatous inflammatory areas were
235 analyzed in a blinded manner. Data are representative images and expressed as the mean \pm
236 SEM of each group (n=8 per group per time point). The survival of remaining mice (n=20 per
237 group) were monitored. **(A)** The gross pathology of the livers from the healthy control **(a)**;
238 infected WT mice **(b)** and ICOS-Tg mice **(c)** and spleens **(d)**: from left to right: normal spleen;
239 infected WT mice; infected ICOS-Tg mice). **(B)** The changes in the liver and spleen weights.
240 The liver and spleen weights of healthy mice at 4 weeks post infection was designated as
241 100%. Two-way ANOVA followed by Tukey's multiple comparison test showed no
242 significant genotype \times time interaction effect for the liver/spleen weight changes ($P=0.455$ /
243 $P=0.16$). The main effects showed a significant difference in the changes of the liver/spleen
244 weights among different time points and different genotypes (** $P<0.01$). **(C)** H&E analysis
245 of the liver sections of mice at 12 weeks post infection. The images are original magnification,
246 $\times 100$; scale bar, 100 μ m. Arrowheads indicate the margins of hepatic granulomatous
247 inflammation. **(D)** The mean granuloma sizes in ICOS-Tg and WT mice were assessed at 7,
248 12, or 16 weeks post-infection and quantified from at least 20 granulomas selected randomly
249 from individual mice, as described in the Materials and Methods. * $P<0.05$, ** $P<0.01$, or
250 *** $P<0.001$ vs. the WT mice. Two-way ANOVA and then Tukey's multiple comparison tests
251 showed a significant genotype \times time interaction effect for the volumes of egg granuloma
252 (* $P<0.05$). The main effects showed a significant difference in the volumes of egg granuloma
253 among different time points and different genotypes (* $P<0.05$ or ** $P<0.01$). **(E)** The survival

254 of mice following *S. japonicum* infection. (ICOS-Tg vs. WT, $P=0.0038$). The survival
255 analysis data are a representative of three independent experiments with similar results.

256

257 **Fig 2. The schistosoma-related liver fibrosis in ICOS-Tg mice.** The liver tissue sections
258 from individual mice at the indicated time points post infection were stained with MT
259 (original magnification $\times 200$). (A) The blue area represents fibrillar collagen. (B) Two-way
260 ANOVA and Tukey's multiple comparison tests showed a significant genotype \times time
261 interaction effect for the ratios of fibrotic to total area (%) (** $P=0.0035$). The main effects
262 showed a significant difference in the ratios of fibrotic to total area (%) among different time
263 points and different genotypes (** $P<0.01$).

264

265 **ICOS over-expression increases the frequency of circulating Tfh cells in mice post-**
266 **infection.**

267 CXCR5⁺Bcl-6⁺Tfh cells can secrete IL-21 and are crucial for humoral responses [9].
268 Recent studies indicate that ICOS positively regulates the Tfh development [8]. To
269 understand the mechanisms underlying the action of ICOS over-expression in this model, we
270 characterized the frequency of circulating Bcl-6⁺CD4⁺, CXCR5⁺CD4⁺ and CXCR5⁺IL-21⁺ T
271 cells in total CD4⁺ T cells in WT and ICOS-Tg mice at different time points post infection by
272 flow cytometry analysis (Fig 3). Quantitative analysis indicated that the percentages of
273 Bcl-6⁺CD4⁺, CXCR5⁺CD4⁺ and CXCR5⁺IL-21⁺ Tfh cells in both strains of mice gradually
274 increased, as compared with that before infection and peaked at 12 weeks post infection,
275 followed by slightly declined. Interestingly, the percentages of Bcl-6⁺CD4⁺, CXCR5⁺CD4⁺

276 and CXCR5⁺IL-21⁺ Tfh cells in the ICOS-Tg mice were significantly higher than that in the
277 WT mice. Similarly, further analysis revealed that the percentages of circulating ICOS⁺
278 CXCR5⁺CD4⁺ and CD40L⁺CXCR5⁺CD4⁺ Tfh cells in the ICOS-Tg mice were significantly
279 higher than that in the WT mice (Fig 4). Hence, induction of systemic ICOS over-expression
280 enhanced Tfh responses in mice following *S. japonicum* infection.

281

282 **Fig 3. The frequency of splenic Tfh cells.** The frequency of splenic Bcl-6⁺CD4⁺ (A),
283 CXCR5⁺CD4⁺ (B) and IL-21⁺CXCR5⁺ (C) Tfh cells in the ICOS-Tg and WT mice was
284 characterized longitudinally post infection by flow cytometry after staining with the indicated
285 antibodies. The cells were first gated on splenic mononuclear cells and at least 10,000 events
286 from each sample were analyzed. Data are representative charts and expressed as the mean ±
287 SEM of the percentages of specific type of Tfh cells in each group (n=5 per group per time
288 point) at the indicated time points post infection from three separate experiments. **P*<0.05,
289 ***P*<0.01, or ****P*<0.001 vs. the WT mice. Two-way ANOVA and Tukey's multiple
290 comparison tests showed a significant genotype × time interaction effect for the Bcl-6
291 (**P*=0.028), CXCR5 (**P*=0.033) and IL-21 (**P*=0.016). The main effects showed a
292 significant difference in the levels of Bcl-6, CXCR5 and IL-21 expression among different
293 genotypes and different times point (**P*<0.05 or ***P*<0.01).

294

295 **Fig 4. The frequency of splenic ICOS⁺ or CD40L⁺ Tfh cells.** The frequency of splenic
296 ICOS⁺CXCR5⁺CD4⁺ Tfh cells and CD40L⁺CXCR5⁺CD4⁺ Tfh cells in the ICOS-Tg and WT
297 mice was characterized by flow cytometry analysis and at least 10,000 events were analyzed.

298 Data are presentative charts and expressed as the mean \pm SEM of the percentages of
299 ICOS⁺CXCR5⁺CD4⁺ Tfh cells (**A**) and CD40L⁺CXCR5⁺CD4⁺ Tfh cells (**B**) in each group
300 (n=5 per group per time point) at the indicated time points post infection from three separate
301 experiments. * P <0.05, ** P <0.01, or *** P <0.001 vs. the WT mice. Two-way ANOVA and
302 Tukey's multiple comparison tests showed a significant genotype \times time interaction effect for
303 the ICOS⁺ Tfh cells (** P =0.001) and CD40L⁺ Tfh cells (* P =0.049). The main effects showed
304 a significant difference in the percentages of ICOS⁺ Tfh cells and CD40L⁺ Tfh cells among
305 different genotypes and different times point (* P <0.05 or** P <0.01).

306

307 **ICOS over-expression promotes antigen-specific Tfh, Th2 and Th17 responses in mice**
308 **post-infection**

309 To further elucidate the role of ICOS-ICOSL signaling in modulating Tfh responses,
310 we isolated splenic mononuclear cells from the ICOS-Tg and WT mice at different time
311 points post *S. japonicum* infection and stimulated them with SEA in the presence or absence
312 of anti-ICOS or anti-ICOSL in vitro, followed by measuring cytokines in the supernatants by
313 CBA. Although the levels of IL-2 and TNF- α increased for a short period post infection in
314 both groups of mice, there was no significant difference in the levels of IL-2 between the
315 ICOS-Tg and WT mice regardless the presence or absence of anti-ICOS or anti-ICOSL (Fig
316 5A and B). Similarly, the levels of IFN- γ also increased for a short period post infection. The
317 levels of IFN- γ in the supernatants of cultured splenic mononuclear cells from the ICOS-Tg
318 mice were significantly lower than that in the WT mice (Fig 5C). The levels of IFN- γ
319 increased dramatically after treatment with anti-ICOS or anti-ICOSL in the supernatants of

320 cultured splenic mononuclear cells from the ICOS-Tg mice, but not from WT mice in most
321 time points tested. Furthermore, the levels of IL-4, IL-10, IL-13, IL-17A, IL-21 and TGF- β 1
322 gradually increased in both groups of mice, peaked at 12 weeks post infection and slightly
323 declined (Fig 5D-I). The levels of IL-4, IL-10, IL-13, IL-17A, IL-21 and TGF- β 1 in the
324 supernatants of cultured splenic mononuclear cells from the ICOS Tg mice were significantly
325 higher than that in the WT mice. Similarly, treatment with anti-ICOS or anti-ICOSL also
326 significantly reduced the levels of IL-4, IL-10, IL-13, IL-17A, IL-21 and TGF- β 1 in the
327 supernatants of cultured splenic mononuclear cells from the ICOS Tg mice (Fig 5D-I). These
328 data clearly demonstrated that induction of systemic ICOS over-expression promoted Tfh,
329 Th2 and Th17 responses in mice infection with *S. japonicum*.

330 Then, we determined the HA titers in ICOS-Tg mice following *S. japonicum* infection
331 and analyzed the potential correlation between the levels of HA and the levels of serum IL-4,
332 IL-13, TGF- β 1, and IL-21 (Fig 6A-D). The levels of serum IL-4, IL-13, and TGF- β 1 were
333 positively correlated with the HA titers in ICOS-Tg mice following *S. japonicum* infection
334 (Fig 6E; $P < 0.01$ or $P < 0.001$). Importantly, the levels of serum IL-21 were also positively
335 correlated with the HA titers in ICOS Tg mice following *S. japonicum* infection ($P < 0.05$)
336 (Fig 6D and E). These data suggest that ICOSL/ICOS interactions play a key role in Tfh, Th2
337 and Th17 responses, which are identified as pertinent to fibrosis.

338

339 **Fig 5. The dynamic changes in the cytokine production by splenocytes from the ICOS-**
340 **Tg and WT mice.** Female ICOS-Tg and WT mice were infected with *S. japonicum*. Splenic
341 mononuclear cells were prepared from each group before and at 4, 7, 12, 16, or 20 weeks

342 post-infection and stimulated in triplicate with SEA, PMA and ionomycin in the presence or
343 absence of anti-ICOS or anti-ICOSL for 72 hrs. The supernatants were harvested and the
344 concentrations of (A) IL-2, (B) TNF- α , (C) IFN- γ , (D) IL-4, (E) IL-10, (F) IL-13, (G)
345 IL-17A, (H) IL-21 and (I) TGF- β 1 were determined by CBA. Data are expressed as the mean
346 \pm SEM of the concentrations of each cytokine in individual group of mice (n=5 per group, per
347 time point) from three independent experiments. ^{3/} $P < 0.05$ between ICOS-Tg and the WT
348 mice, ¹ $P < 0.05$ between ICOS-Tg and Tg-ICOSL-blocking mice, [▼] $P < 0.05$ between ICOS-Tg
349 and Tg-ICOS-blocking mice. Two-way ANOVA and Tukey's multiple comparison tests
350 showed a significant genotype \times time interaction effect for the IFN- γ (* $P=0.046$), IL-4
351 (** $P=0.005$), IL-10 (* $P=0.031$), IL-13 (** $P < 0.01$), IL-17A (* $P=0.038$), IL-21 (* $P=0.028$)
352 and TGF- β 1 (** $P=0.004$). The main effects showed a significant difference among different
353 genotypes and different time points in the level of IL-2, TNF- α , IFN- γ , IL-4, IL-10, IL-13,
354 IL-17A, IL-21 and TGF- β 1 (* $P < 0.05$ or ** $P < 0.01$).

355

356 **Fig 6. The analysis of correlation of Th2 / Tfh and fibrosis.** The linear relationship of IL-4
357 (A: $R=0.4727$, ** $P=0.0083$), IL-13 (B: $R=0.5306$, ** $P=0.0026$), TGF- β 1 (C: $R=0.5858$,
358 *** $P=0.0007$), IL-21 (D: $R=0.4234$, * $P=0.0197$) and HA. The results are a representative of
359 three independent experiments with similar results, which are from 6 time points (at 0, 4, 7,
360 12, 16, 20 weeks) (E). The comparison of Spearman R from the analysis of correlation. The
361 Spearman R from the analysis of correlation between IL-4 / IL-13 / TGF- β 1 / IL-21 and HA.
362 * $P < 0.05$, ** $P < 0.01$, and *** $P < 0.001$ between cytokine and HA, Spearman's rank.

363

364 **ICOS over-expression enhances antigen-specific humoral responses and Tfh liver**

365 **infiltration in mice post-infection.**

366 Tfh cells can promote humoral response. Finally, we assessed the impact of systemic
367 ICOS over-expression on SEA-specific humoral responses and on the degrees of liver Tfh
368 infiltration in mice at different time points post *S. japonicum* infection. We found that *S.*
369 *japonicum* infection induced SEA-specific IgG responses, which gradually increased and
370 peaked at 12 weeks post infection in both groups of mice. The levels of serum SEA-specific
371 IgG in the ICOS-Tg mice were significantly higher than that in the WT mice at chronic stage
372 of *S. japonicum* infection (Fig 7A). Immunohistochemistry analyses indicated that the
373 intensity and extensity of positively anti-BCL-6 and anti-CXCR5 staining in the liver sections
374 of ICOS-Tg mice were obviously stronger than that in the WT mice at 12 weeks post
375 infection (Fig 7B). Quantitative analysis revealed that the ratios of IOD to AOV1 for
376 anti-Bcl-6 and anti-CXCR5 staining in the livers of ICOS Tg mice were significantly greater
377 than that in the WT mice at 12 weeks post infection (Fig 7C). Therefore, these data clearly
378 indicated that induction of systemic ICOS over-expression promoted antigen-specific
379 humoral responses and Tfh liver infiltration in mice following *S. japonicum* infection.

380

381 **Fig 7. The concentrations of serum SEA-specific IgG and the intensity of Tfh liver**

382 **infiltration liver in mice.** The concentrations of serum anti-SEA IgG in the ICOS-Tg and
383 WT mice at the indicated time points post infection were determined by ELISA (A) and the
384 degrees of Tfh infiltrates in the livers of both groups of mice at 12 weeks post infection were
385 determined by immunohistochemistry using anti-Bcl-6 and anti-CXCR5 (B). The intensity of

386 anti-Bcl-6 and anti-CXCR5 staining was analyzed by the % positively staining cells in 15
387 granulomas (C). Data are representative images and expressed as the mean \pm SEM of the
388 concentrations of serum IgG and the mean of % positively staining cells in 15 granulomas +/-
389 SD of each group of mice (n=5 per group per time point) from three separate experiments.
390 * P <0.05, ** P <0.01, or *** P <0.001 vs. the WT mice. Two-way ANOVA and Tukey's
391 multiple comparison tests showed no significant genotype \times time interaction effect for the
392 concentrations of serum anti-SEA IgG (P =0.08). The main effects showed a significant
393 difference in the changes of the liver/spleen weights among different time points and different
394 genotypes (** P <0.01).

395

396 **Discussion**

397 Tfh cells are crucial for B cell activation, germinal center formation and humoral
398 responses [7]. ICOS, besides CD40L and CD28, is important for T cell activation,
399 particularly for Tfh cells. In this study, we tested the impact of systemic ICOS over-
400 expression on the dynamics of liver granulomatous inflammation and fibrosis in mice
401 following *S. japonicum* infection. We found that in comparison with that in the WT mice,
402 larger liver and spleens organs and greater wet liver and spleen weights were observed,
403 accompanied by significantly severer liver granulomatous inflammation and fibrosis in the
404 ICOS-Tg mice. As a result, the ICOS-Tg mice had significantly shorter survival following *S.*
405 *japonicum* infection. Clearly, these data demonstrated that systemic ICOS over-expression
406 promoted the liver granulomatous inflammation, fibrosis and mortality in mice following *S.*
407 *japonicum* infection. These novel findings indicated that systemic ICOS over-expression not

408 only promoted the liver granulomatous inflammation and fibrosis, but also accelerated the
409 mortality in *S. japonicum*-infected mice.

410 Recent studies have shown that the ICOS signaling can promote Tfh cell differentiation
411 and IL-21 production [9,10]. To understand the mechanisms underlying the action of ICOS
412 over-expression, we characterized the frequency of splenic Tfh cells in the ICOS-Tg and WT
413 mice following *S. japonicum* infection. We found that the percentages of Bcl-6⁺CD4⁺,
414 CXCR5⁺CD4⁺, CXCR5⁺IL-21⁺ and CD40L⁺CXCR5⁺CD4⁺ Tfh cells gradually increased in
415 both groups of mice following *S. japonicum* infection and the percentages of these Tfh cells
416 in the ICOS-Tg mice were significantly higher than that in the WT mice. These data indicated
417 that ICOS enhanced Tfh development during the process of *S. japonicum* infection. It is
418 possible that ICOS may up-regulate the CXCR5 and Bcl-6 expression to promote the
419 differentiation of Tfh cells. More importantly, we observed significantly higher levels of
420 IL-21 secreted by splenic mononuclear cells from ICOS-Tg mice following *S. japonicum*
421 infection. Given that IL-21 is a growth factor and important for the function of Tfh cells, it is
422 possible that the ICOS signaling may also enhance IL-21 expression, providing a positive
423 feedback regulation of Tfh responses. The higher frequency of Tfh cells, the higher levels of
424 IL-21 production may activate and expand memory B cells, thereby enhancing humoral
425 responses. Indeed, we detected significantly higher levels of SEA-specific humoral responses
426 in the ICOS-Tg mice. Apparently, ICOS through promoting Tfh development and in turn
427 enhancing humoral responses, contributes to the pathogenesis of granulomatous inflammation
428 and fibrosis in mice following *S. japonicum* infection. Potentially, ICOS and Tfh may be
429 immune check points for the prevention and intervention of *Schistosoma*-related

430 granulomatous inflammation and fibrosis.

431 It is well known that Th2 and Th17 responses are involved in the pathogenesis of
432 *Schistosoma*-related granulomatous inflammation and fibrosis. In this study, we found that
433 significantly higher levels of SEA-specific Th2 and Th17 responses in the ICOS-Tg mice,
434 which was abrogated by treatment with a blocker of the ICOS/ICOSL signaling. These data
435 suggest that the ICOS signaling may promote Th2 and Th17 responses during the pathogenic
436 process of *Schistosoma*-related granulomatous inflammation and fibrosis. Our findings were
437 consistent with previous observations that the ICOS expands Th2 immunity and Th2-
438 mediated inflammation by augmenting the migration of inflammatory infiltrates [25,26].
439 Interestingly, we also detected significantly higher levels of IL-10 and TGF- β 1 responses in
440 the ICOS-Tg mice. Given that IL-10 and TGF- β 1 are important anti-inflammatory cytokines
441 secreted by regulatory T cells (Tregs), the enhanced anti-inflammatory responses may inhibit
442 the liver granulomatous inflammation. Hence, the ICOS signaling has dual functions by
443 promoting pathogenic Th2 and Th17 responses and enhancing anti-inflammatory IL-10 and
444 TGF- β 1 responses during the pathogenesis of *Schistosoma*-related granulomatous
445 inflammation. Unfortunately, TGF- β 1 is potent pro-fibrotic factor and through its receptor to
446 activate the Smad signaling to promote fibrosis-related gene expression [27,28]. It is possible
447 that the ICOS signaling through enhancing TGF- β 1 production contributes to the
448 pathogenesis of *Schistosoma*-related liver fibrosis. Therefore, inhibition of the ICOS
449 signaling may not only attenuate hepatic granulomatous inflammation, but also mitigate
450 *Schistosoma*-related liver fibrosis.

451 In summary, our data indicated that systemic ICOS over-expression deteriorated the

452 pathogenic process of *Schistosoma*-related liver granulomatous inflammation and fibrosis and
453 accelerated mortality in mice. Furthermore, systemic ICOS over-expression not only
454 significantly increased the frequency of splenic Tfh cells, but also enhanced SEA-specific
455 Th2, Th17, IgG, IL-21, IL-10 and TGF- β 1 responses in mice following *S. japonicum*
456 infection. Hence, the ICOS signaling has sequential roles in regulating the *Schistosoma*-
457 related liver granulomatous inflammation and fibrosis in mice. Importantly, the ICOS
458 signaling may be an immune check point for the prevention and intervention of *Schistosoma*-
459 related liver granulomatous inflammation and fibrosis. Therefore, our findings may not only
460 provide new insights into the mechanisms by which the ICOS regulates the pathogenesis of
461 *Schistosoma*-related liver granulomatous inflammation and fibrosis, but also may aid in the
462 design of new therapies for the intervention of *Schistosoma*-induced fibrosis.

463

464

465 **References**

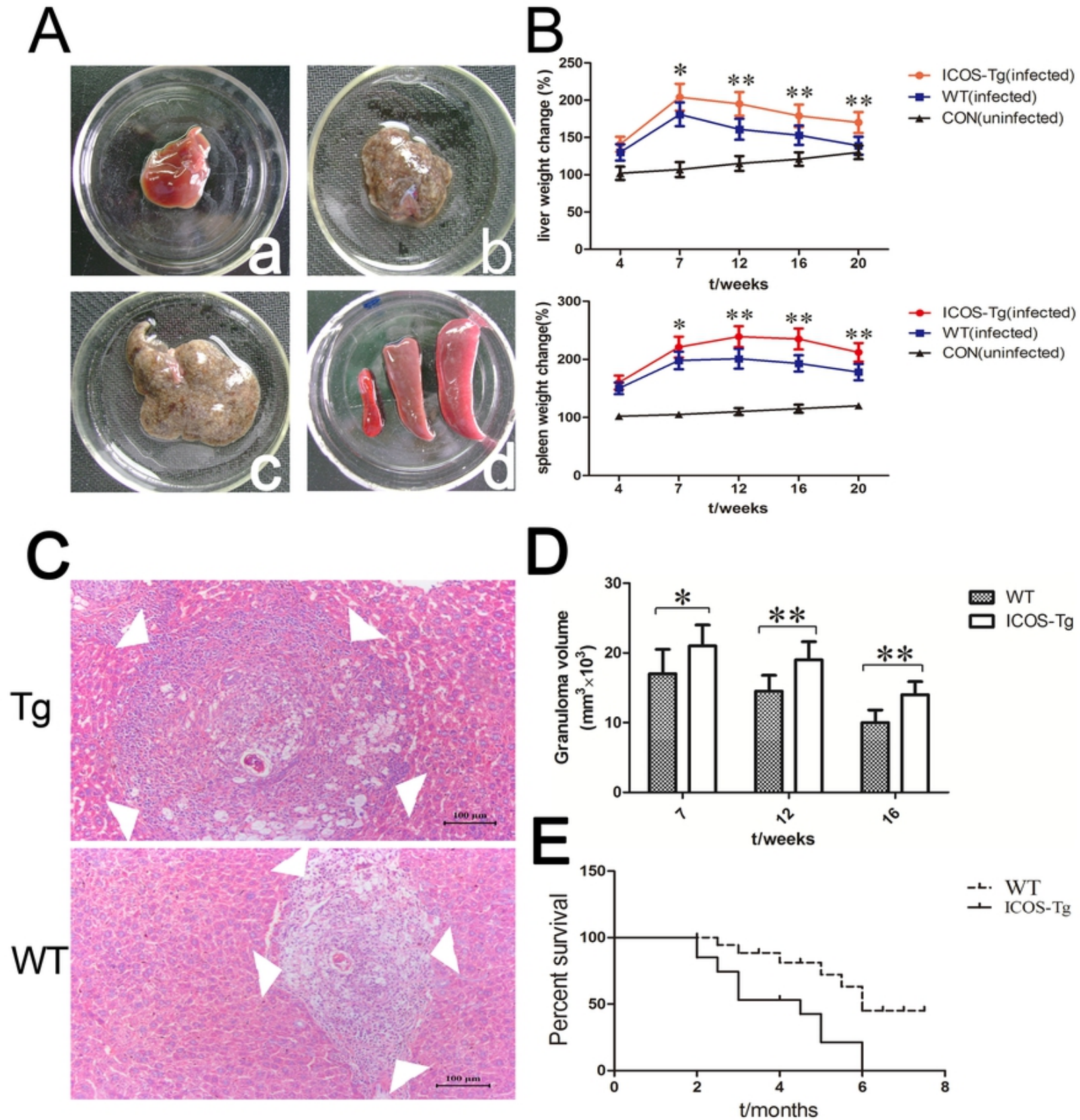
- 466 1. Nono JK, Ndlovu H, Aziz NA, Mpotje T, Hlaka L, Brombacher F. Host regulation of
467 liver fibroproliferative pathology during experimental schistosomiasis via interleukin-4
468 receptor alpha. *PLoS Negl Trop Dis*. 2017 Aug 21;11(8):e0005861. doi:
469 10.1371/journal.pntd.0005861. PMID: 28827803; PMCID: PMC5578697.
- 470 2. Vicentino ARR, Carneiro VC, Allonso D, Guilherme RF, Benjamim CF, Vicentino ARR,
471 et al. Emerging Role of HMGB1 in the pathogenesis of schistosomiasis liver fibrosis.
472 *Front Immunol*. 2018 Sep 12;9:1979. doi: 10.3389/fimmu.2018.01979. PMID:
473 30258438; PMCID: PMC6143665.
- 474 3. Kumar R, Mickael C, Kassa B, Sanders L, Koyanagi D, Hernandez-Saavedra D, et al.
475 Th2 CD4+ T Cells are necessary and sufficient for Schistosoma-pulmonary
476 hypertension. *J Am Heart Assoc*. 2019 Aug 6;8(15):e013111. doi: 10.1161/JAHA.
477 119.013111. Epub 2019 Jul 24. PMID: 31339057; PMCID: PMC6761627.
- 478 4. Soloviova K, Fox EC, Dalton JP, Caffrey CR, Davies SJ. A secreted schistosome
479 cathepsin B1 cysteine protease and acute schistosome infection induce a transient T
480 helper 17 response. *PLoS Negl Trop Dis*. 2019 Jan 17;13(1): e0007070. doi: 10.1371/
481 journal.pntd.0007070. PMID: 30653492; PMCID: PMC6353221.
- 482 5. Wang B, Liang S, Wang Y, Zhu XQ, Gong W, Zhang HQ, et al. Th17 down-regulation
483 is involved in reduced progression of schistosomiasis fibrosis in ICOSL KO mice.
484 *PLoS Negl Trop Dis*. 2015 Jan 15;9(1):e0003434. doi: 10.1371/journal.pntd.0003434.
485 PMID: 25590646; PMCID: PMC4295877.
- 486 6. Qin L, Waseem TC, Sahoo A, Bieberkehazhi S, Zhou H, Galkina EV, et al. Insights into

- 487 the molecular mechanisms of T follicular helper-mediated immunity and pathology.
488 Front Immunol. 2018 Aug 15;9:1884. doi: 10.3389/fimmu.2018.01884. PMID:
489 30158933; PMCID: PMC6104131.
- 490 7. Wu H, Deng Y, Zhao M, Zhang J, Zheng M, Chen G, et al. Molecular control of
491 follicular helper T cell development and differentiation. Front Immunol. 2018 Oct
492 25;9:2470. doi: 10.3389/fimmu.2018.02470. PMID: 30410493; PMCID:
493 PMC6209674.
- 494 8. Uwadiae FI, Pyle CJ, Walker SA, Lloyd CM, Harker JA. Targeting the ICOS/ICOS-L
495 pathway in a mouse model of established allergic asthma disrupts T follicular helper
496 cell responses and ameliorates disease. Allergy. 2019 Apr;74(4):650-662. doi: 10.1111/
497 all.13602. Epub 2018 Nov 12. PMID: 30220084; PMCID: PMC6492018.
- 498 9. Wang Y, Lin C, Cao Y, Duan Z, Guan Z, Xu J, et al. Up-regulation of interleukin-21
499 contributes to liver pathology of schistosomiasis by driving GC immune responses and
500 activating HSCs in mice. Sci Rep. 2017 Nov 30;7(1):16682. doi: 10.1038/
501 s41598-017-16783-7. PMID: 29192177; PMCID: PMC5709429.
- 502 10. Shi J, Hou S, Fang Q, Liu X, Liu X, Qi H. PD-1 controls follicular T helper cell
503 positioning and function. Immunity. 2018 Aug 21;49(2):264-274.e4. doi: 10.1016/
504 j.immuni.2018.06.012. Epub 2018 Jul 31. PMID: 30076099; PMCID: PMC6104813.
- 505 11. Read KA, Powell MD, Oestreich KJ. T follicular helper cell programming by
506 cytokine-mediated events. Immunology. 2016 Nov;149(3):253-261. doi:10.1111/
507 imm.12648. Epub 2016 Aug 16. PMID: 27442976; PMCID: PMC5046059.
- 508 12. Kim ST, Choi JY, Lainez B, Schulz VP, Karas DE, Baum ED, et al. Human

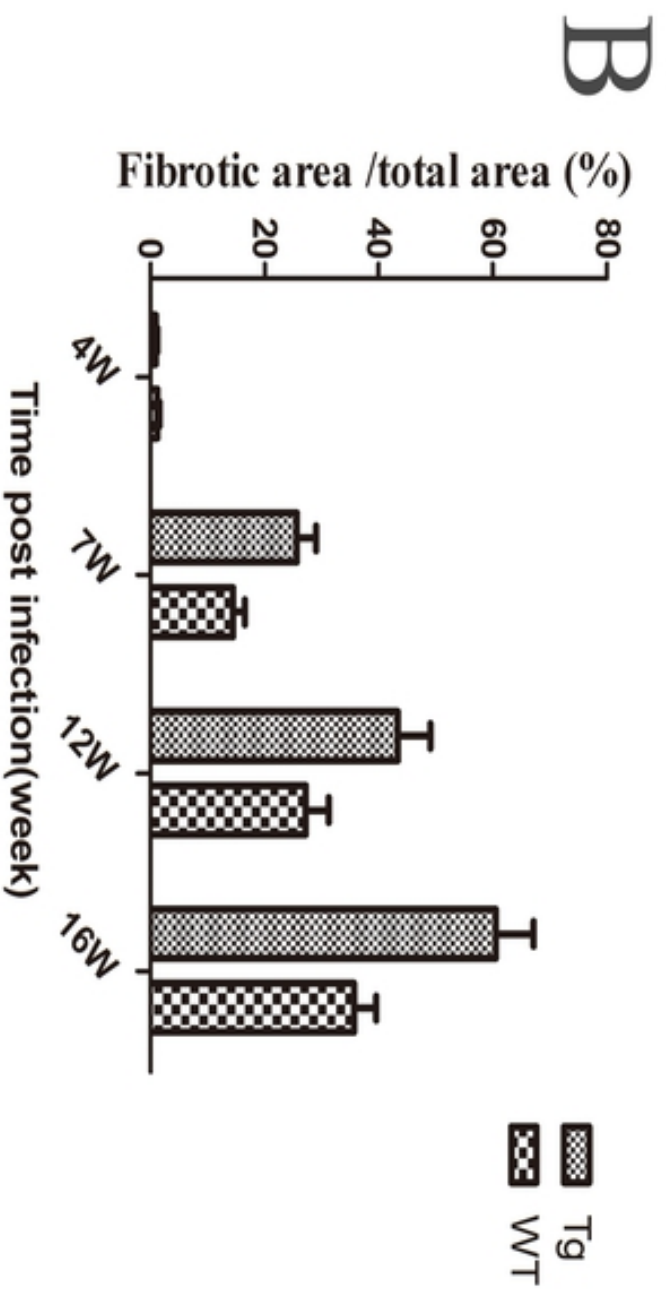
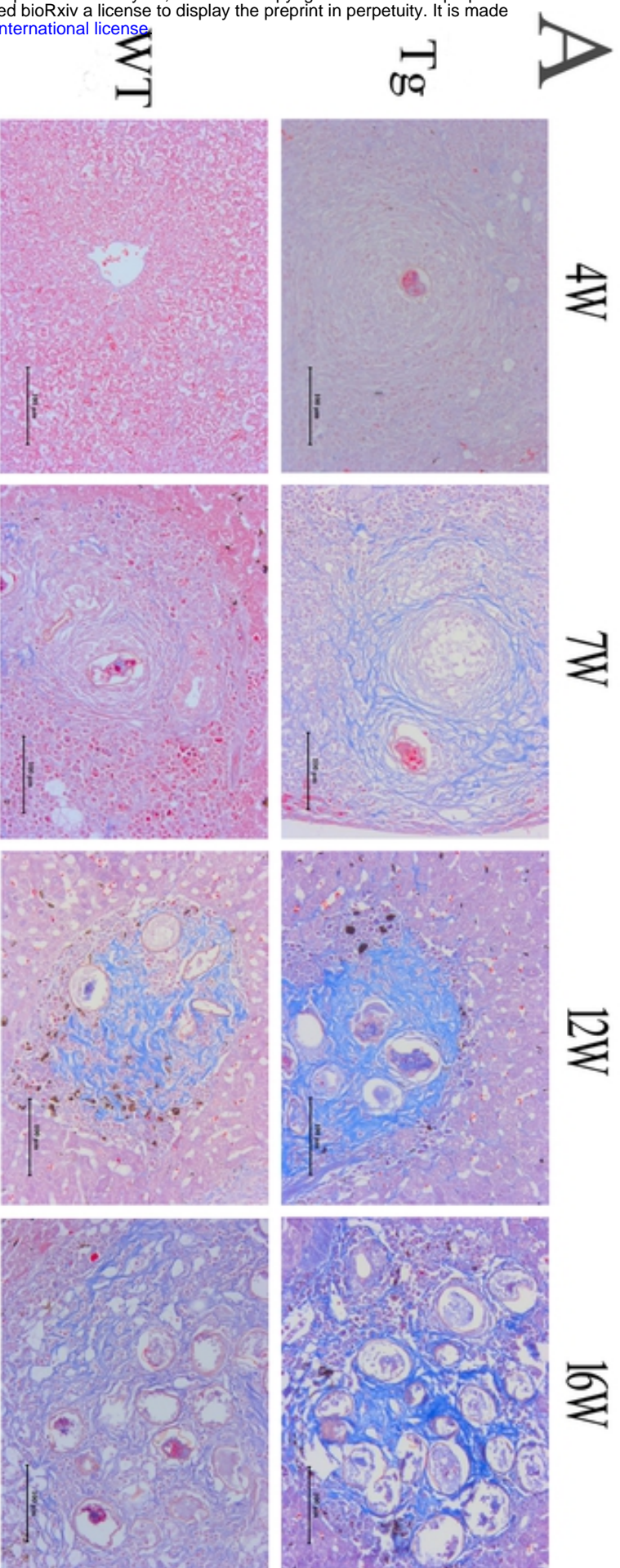
- 509 extrafollicular CD4⁺ Th cells help memory B cells produce Igs. *J Immunol.* 2018 Sep
510 1;201(5):1359-1372. doi: 10.4049/jimmunol.1701217. Epub 2018 Jul 20. PMID:
511 30030323; PMCID: PMC6112860.
- 512 13. Xie MM, Dent AL. Unexpected Help: Follicular regulatory T cells in the germinal
513 center. *Front Immunol.* 2018 Jul 2;9:1536. doi: 10.3389/fimmu.2018.01536. PMID:
514 30013575; PMCID: PMC6036241.
- 515 14. Gensous N, Charrier M, Duluc D, Contin-Bordes C, Truchetet ME, Lazaro E, et al. T
516 follicular helper cells in autoimmune disorders. *Front Immunol.* 2018 Jul 17;9: 1637.
517 doi: 10.3389/fimmu.2018.01637. PMID: 30065726; PMCID: PMC6056609.
- 518 15. Quinn JL, Axtell RC. Emerging role of follicular T helper cells in multiple sclerosis
519 and experimental autoimmune encephalomyelitis. *Int J Mol Sci.* 2018 Oct 19;19(10):
520 3233. doi: 10.3390/ijms19103233. PMID: 30347676; PMCID: PMC6214126.
- 521 16. Cao G, Chi S, Wang X, Sun J, Zhang Y. CD4⁺CXCR5⁺PD-1⁺ T follicular helper cells
522 play a pivotal role in the development of rheumatoid arthritis. *Med Sci Monit.* 2019
523 Apr 25;25:3032-3040. doi:10.12659/MSM.914868. PMID: 31019190; PMCID:
524 PMC6498883.
- 525 17. Chen X, Li W, Zhang Y, Song X, Xu L, Xu Z, et al. Distribution of peripheral memory
526 T follicular helper cells in patients with schistosomiasis Japonica. *PLoS Negl Trop*
527 *Dis.* 2015 Aug 18;9(8):e0004015. doi: 10.1371/journal.pntd.0004015. PMID:
528 26284362; PMCID: PMC4540279.
- 529 18. Zhang Y, Wang Y, Jiang Y, Pan W, Liu H, Yin J, et al. T follicular helper cells in
530 patients with acute schistosomiasis. *Parasit Vectors.* 2016 Jun 6;9(1):321. doi:10.1186/

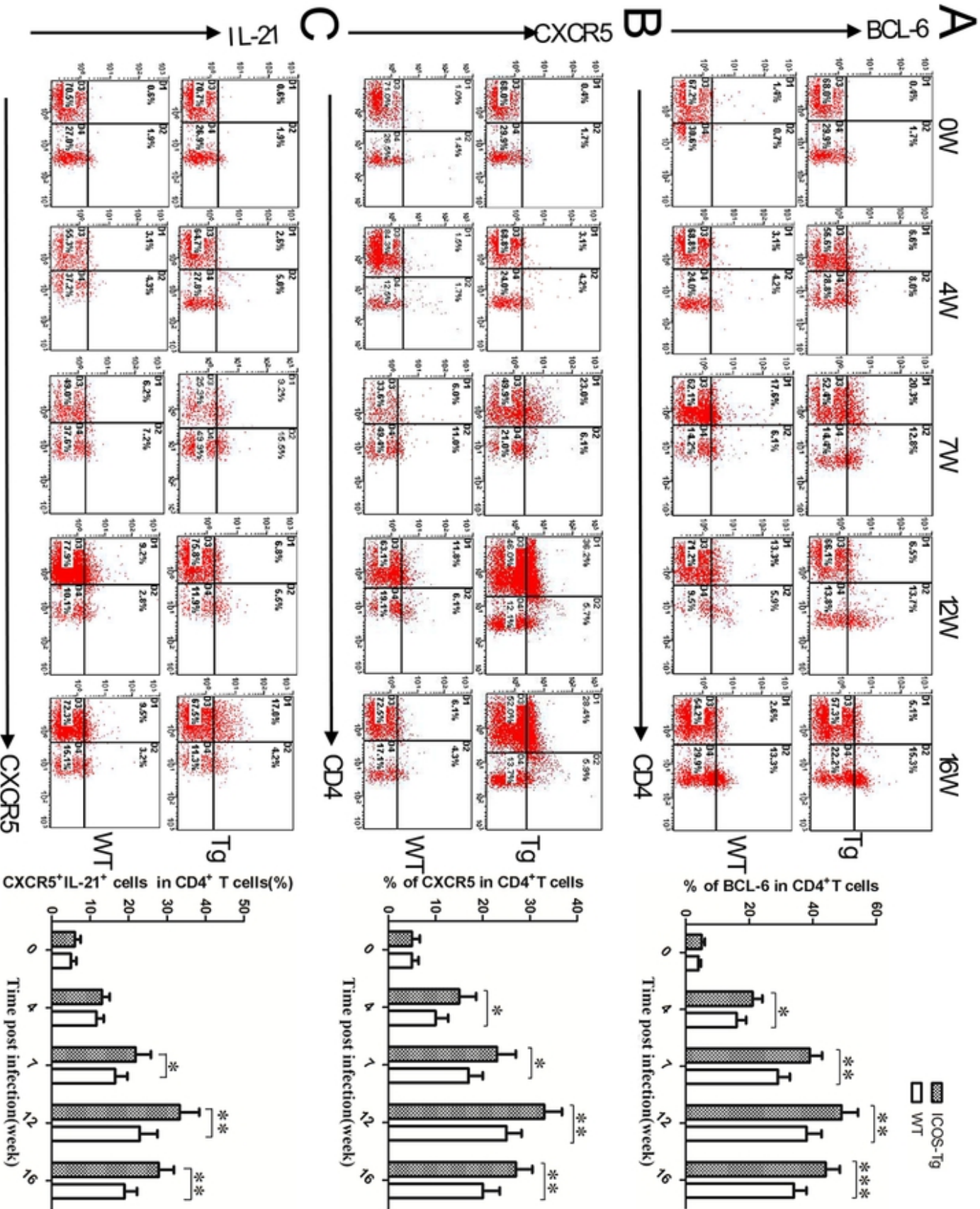
- 531 s13071-016-1602-6. PMID: 27266984; PMCID: PMC4895967.
- 532 19. Chen X, Yang X, Li Y, Zhu J, Zhou S, Xu Z, et al. Follicular helper T cells promote
533 liver pathology in mice during *Schistosoma japonicum* infection. PLoS Pathog. 2014
534 May 1;10(5):e1004097. doi: 10.1371/journal.ppat.1004097. PMID: 24788758;
535 PMCID: PMC4006917.
- 536 20. Wikenheiser DJ, Stumhofer JS. ICOS co-stimulation: friend or foe? Front Immunol.
537 2016 Aug 10;7:304. doi: 10.3389/fimmu.2016.00304. PMID: 27559335; PMCID:
538 PMC4979228.
- 539 21. Le KS, Amé-Thomas P, Tarte K, Gondois-Rey F, Granjeaud S, Orlanducci F, et al.
540 CXCR5 and ICOS expression identifies a CD8 T-cell subset with T_{FH} features in
541 Hodgkin lymphomas. Blood Adv. 2018 Aug 14;2(15): 1889-1900. doi: 10.1182/
542 bloodadvances.2018017244. PMID: 30087107; PMCID: PMC6093730.
- 543 22. Liu J, Zhou Y, Yu Q, Zhao Z, Wang H, Luo X, et al. Higher Frequency of
544 CD4+CXCR5+ICOS+PD1+ T follicular helper cells in patients with infectious
545 mononucleosis. Medicine (Baltimore). 2015 Nov;94(45):e2061. doi: 10.1097/MD.
546 0000000000002061. PMID: 26559315; PMCID: PMC4912309.
- 547 23. Jogdand GM, Sengupta S, Bhattacharya G, Singh SK, Barik PK, Devadas S. Inducible
548 costimulator expressing T cells promote parasitic growth during blood
549 stage *plasmodium berghei* ANKA infection. Front Immunol. 2018 May 28;9:1041. doi:
550 10.3389/fimmu.2018.01041. PMID: 29892278; PMCID: PMC5985291.
- 551 24. Wikenheiser DJ, Ghosh D, Kennedy B, Stumhofer JS. The costimulatory molecule
552 ICOS regulates host Th1 and follicular Th Cell differentiation in response to

- 553 plasmodium chabaudi chabaudi AS infection. *J Immunol.* 2016 Jan 15;196(2):778-91.
554 doi: 10.4049/jimmunol.1403206. Epub 2015 Dec 14. PMID: 26667167; PMCID:
555 PMC4705592.
- 556 25. Tesciuba AG, Shilling RA, Agarwal MD, Bandukwala HS, Clay BS, Moore TV, et al.
557 ICOS costimulation expands Th2 immunity by augmenting migration of lymphocytes
558 to draining lymph nodes. *J Immunol.* 2008 Jul 15;181(2):1019- 24. doi: 10.4049/
559 jimmunol.181.2.1019. PMID: 18606653; PMCID: PMC2560985.
- 560 26. Shilling RA, Clay BS, Tesciuba AG, Berry EL, Lu T, Moore TV, et al. CD28 and ICOS
561 play complementary non-overlapping roles in the development of Th2 immunity in
562 vivo. *Cell Immunol.* 2009;259(2):177-84. doi:10.1016/j.cellimm.2009.06.013. Epub
563 2009 Jul 10. PMID: 19646680; PMCID: PMC2748173.
- 564 27. Ahamed J, Laurence J. Role of platelet-derived transforming growth factor- β 1 and
565 reactive oxygen species in radiation-induced organ fibrosis. *Antioxid Redox Signal.*
566 2017 Nov 1;27(13):977-988. doi: 10.1089/ars. 2017.7064. Epub 2017 Jul 5. PMID:
567 28562065; PMCID: PMC5649128.
- 568 28. Jee MH, Hong KY, Park JH, Lee JS, Kim HS, Lee SH, et al. New mechanism of
569 hepatic fibrogenesis: hepatitis C virus infection induces transforming growth factor β 1
570 production through glucose-regulated protein 94. *J Virol.* 2015 Dec 30;90(6):3044-55.
571 doi: 10.1128/JVI.02976-15. PMID: 26719248; PMCID: PMC4810663.

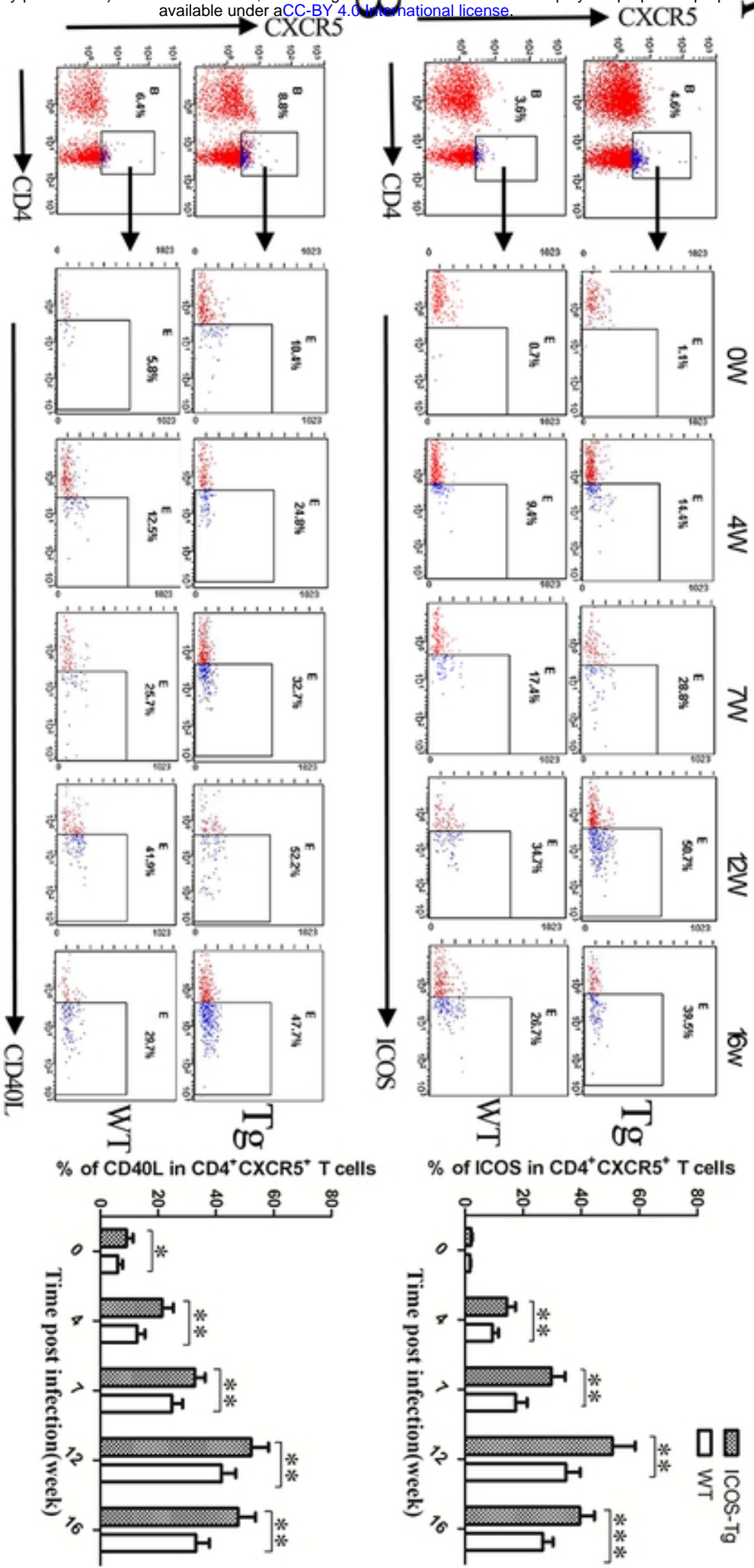


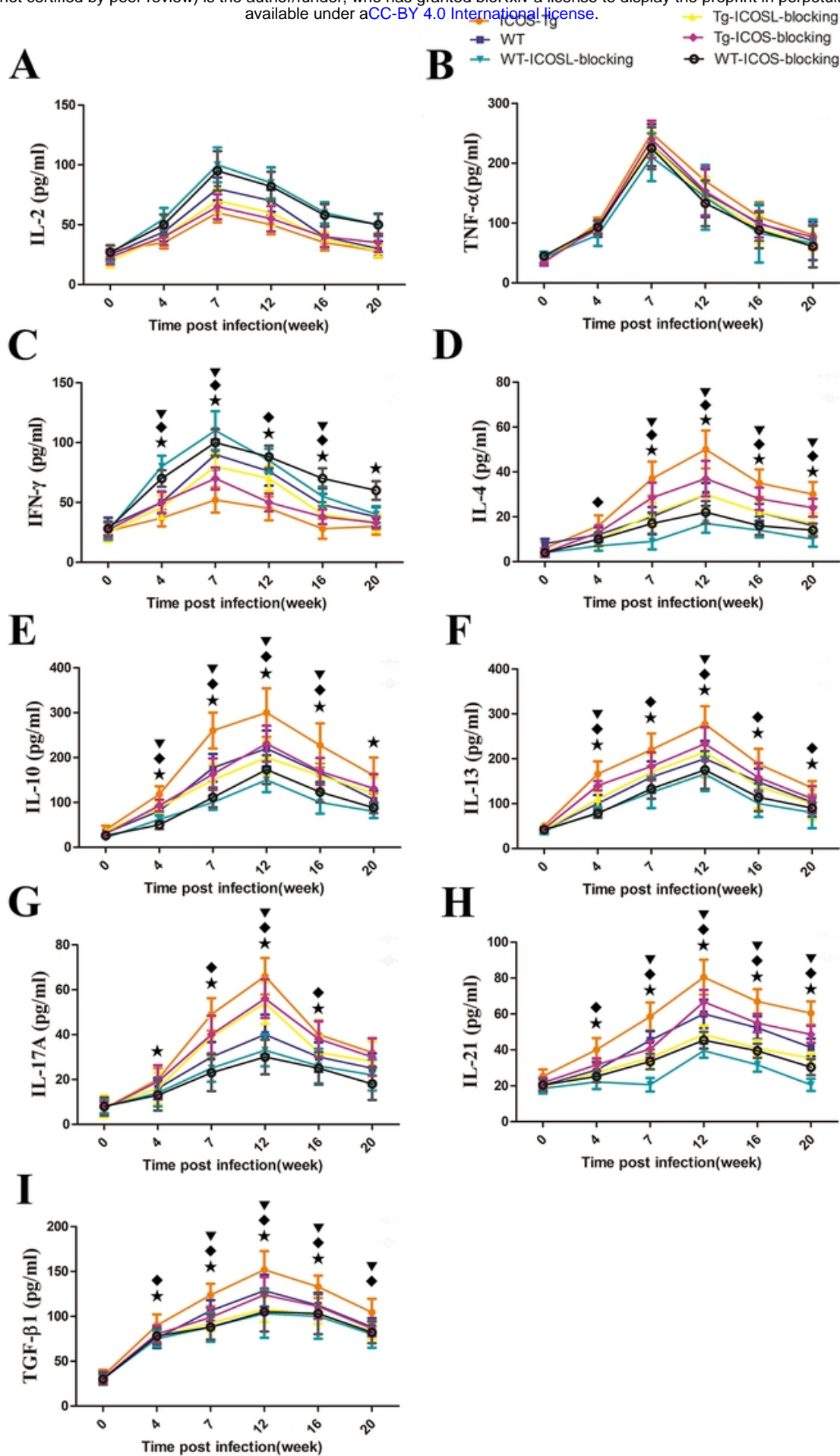
Figure



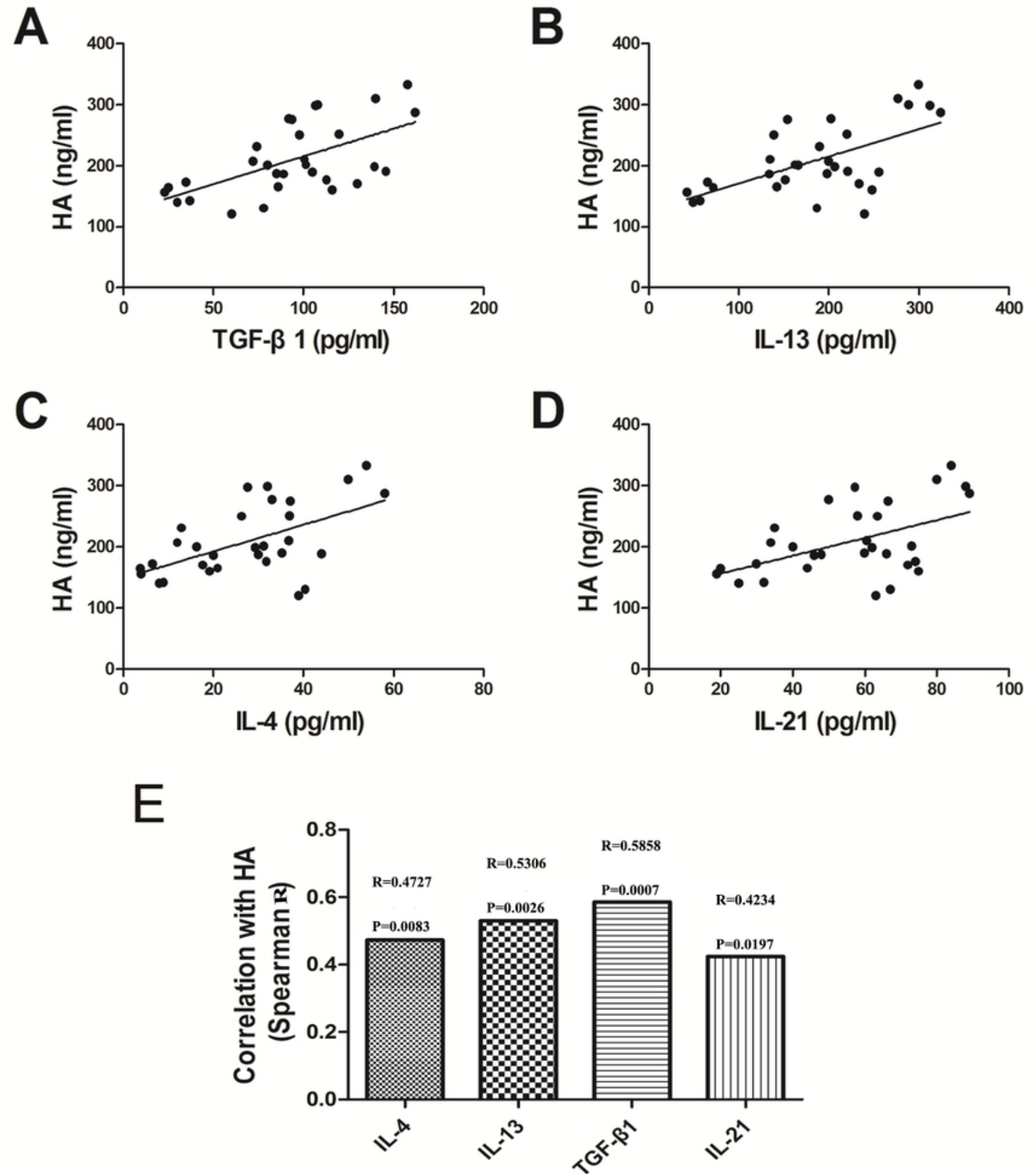


Figure



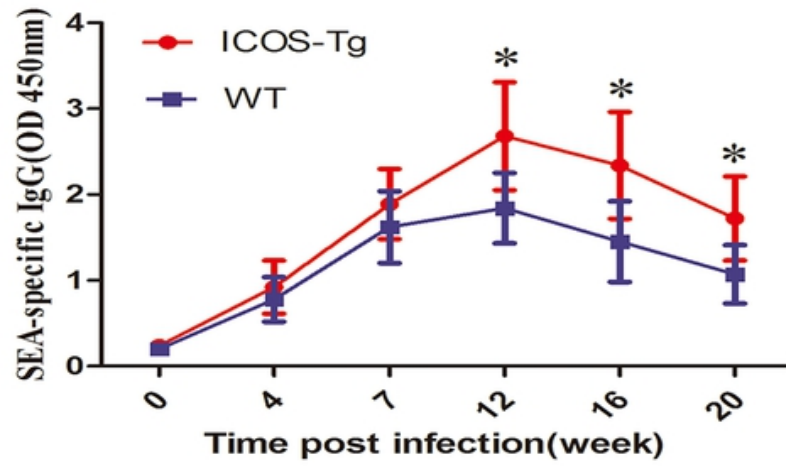


Figure

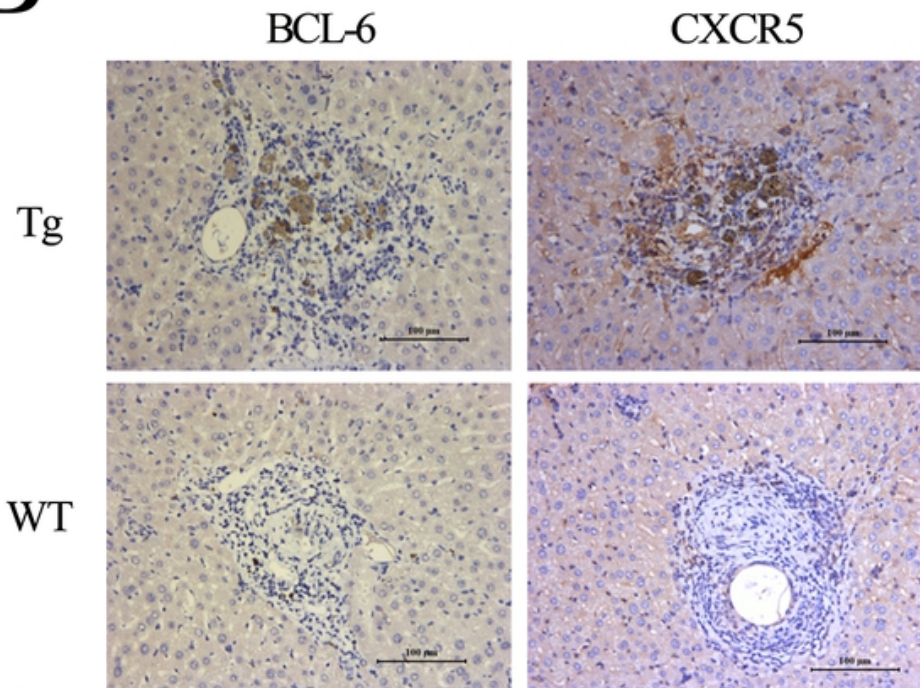


Figure

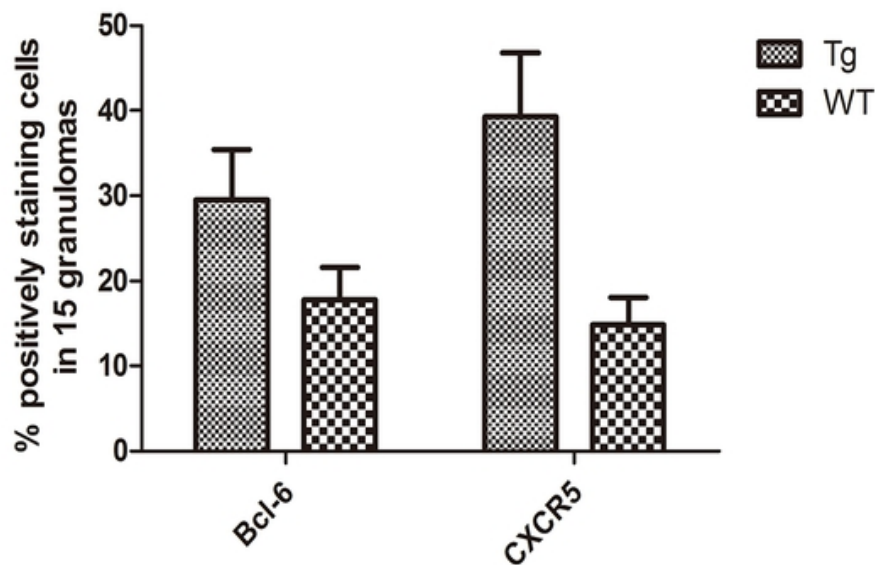
A



B



C



Figure